Progress In Electromagnetics Research Letters, Vol. 52, 23–30, 2015

A Dual-Frequency Matching Network for FDCLs Using Dual-Band $\lambda/4$-Lines

Mohammad A. Maktoomi[1, *], Mohammad S. Hashmi[1, 2], and Vipul Panwar[1]

Abstract—A new approach to design a dual-band matching network using a dual-band quarter-wave line is presented. The proposed matching network is capable of simultaneously matching frequency-dependent complex loads (FDCLs) having different values at two arbitrary frequencies to a real source impedance, Z_0. A very simple step-wise design procedure is discussed for the transformer along with closed-form design equations which are very simple in nature. For experimental verification, two PCB prototypes have been fabricated using FR-4 material, operating at 1 GHz and 2.42 GHz. The measurements results matches well with that obtained from simulation, exhibiting good performance.

1. INTRODUCTION

Impedance matching is one of the fundamental tasks in RF/Microwave circuit design. They find applications in amplifiers, mixers, oscillators, antennas and power splitters/combiners. Traditional quarter-wavelength/single-/double-stub impedance transformers are routinely used for this purpose [1].

With the growing interests in dual-band/multi-band circuits and systems, requirement of matching networks operating at two/multi-frequencies has emerged. Thus, many dual-frequency matching networks have been reported. For instance, real load impedance to real source impedance dual frequency transformer was reported in [2], Chebyshev impedance transformer was reported in [3], an L-type transformer was reported in [4], and an impedance transformer with a DC block property was presented in [5].

However, a more general and interesting problem is the situation where the load may be complex as well as frequency dependent (that is, different complex impedances at two distinct frequencies). To match such FDCLs many circuits have been reported, for example in [6–9].

In this paper, a new approach to design dual-band matching circuit is presented which is generic and intuitive in nature. One of the possible circuit architectures is implemented to demonstrate the underlying concept behind the proposed technique. The designed circuit is simulated in Agilent ADS and two prototypes are manufactured to compare the experimental and simulated results.

2. PROPOSED MATCHING NETWORK: BASIC IDEA

The basic structure of proposed transformer is shown in Figure 1. The FDCL is assumed to have values as $Z_L = R_1 + jX_1 \,@\, f_1$ and $Z_L = R_2 + jX_2 \,@\, f_2$. Y_{in1} is the admittance looking into Section A, Y_{in2} is the admittance looking into Section B whereas Z_{in3} is the impedance looking into the combination of Section A and Section B.

Received 4 February 2015, Accepted 17 February 2015, Scheduled 5 March 2015

* Corresponding author: Mohammad A. Maktoomi (ayatullahm@iiitd.ac.in).

[1] Wireless Systems Lab, Department of Electronics and Communications Engineering, IIIT-Delhi, New Delhi 110020, India. [2] iRadio Lab, Department of Electrical and Computer Engineering, Schulich School of Engineering, University of Calgary, Calgary, Alberta T2N 1N4, Canada.

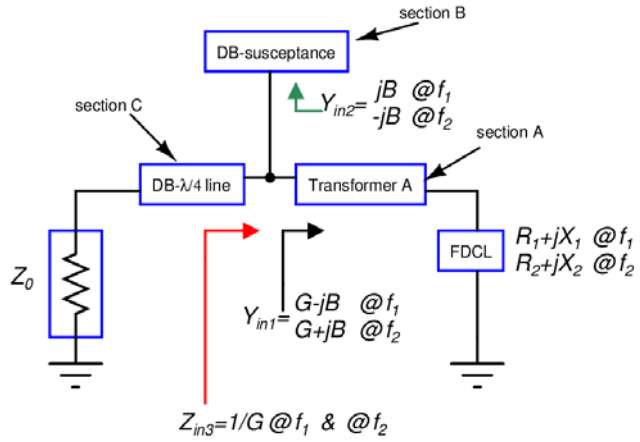

Figure 1. Pictorial illustration of the proposed matching scheme (DB: dual-band).

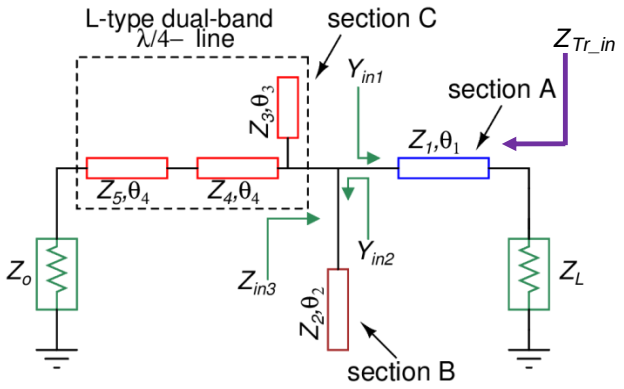

Figure 2. Implemented dual-frequency matching network based on scheme shown in Figure 1.

It is apparent from Figure 1 that transformer A converts the FDCL to produce Y_{in1} such that $Y_{in1}|_{f_1} = Y^*_{in1}|_{f_2}$, that is, if $Y_{in1}|_{f_1} = G - jB$ then $Y_{in1}|_{f_2} = G + jB$. Section B, which is primarily a dual-band susceptance, cancels out the imaginary parts of Y_{in1} at the two specified frequencies. Thus, as a last step there is a need to match $Z_{in3} = 1/G$ to Z_0 at the two frequencies. It is well known that a real impedance (such as Z_{in3}) can be matched to another real impedance (such as Z_0) using a $\lambda/4$ line; the only additional requirement in the present case is to have a dual-band $\lambda/4$ line which is what Section C essentially is.

It must be noted at this juncture that most of the previously reported schemes have used Section A and Section B in the same manner as being used here. The main aspect of the proposed scheme is the incorporation of dual-band $\lambda/4$ line into the conventional structure. The strength and uniqueness of the proposed impedance network, therefore, is the flexibility of choosing any dual-band $\lambda/4$-line from a variety of those reported in the literature to suit specific applications [10, 11].

3. IMPLEMENTATION OF THE TRANSFORMER

One possible implementation of the proposed matching network is shown in Figure 2. Section A, adjacent to the FDCL ($Z_L = R_1 + jX_1$ at f_1 and $R_2 + jX_2$ at f_2) is a transmission line having characteristic impedance Z_1 and electrical length θ_1. Section B is either a short or an open stub having characteristic impedance Z_2 and electrical length θ_2 whereas Section C is an L-shaped dual-band $\lambda/4$-line. The term Z_{Tr_in} is the input impedance that the load sees into the transformer.

Design equations for Sections A and B are detailed in [9], but for the sake of completeness they are discussed briefly in Subsections 3.1 and 3.2, respectively. Finally, design of Section C is discussed in Subsection 3.3.

3.1. Design of Section A

The required values of Z_1 and θ_1 and resulting values of G and B, given in the following expressions, may be deduced from the results given in [6]:

$$Z_1 = \sqrt{R_1R_2 + X_1X_2 + \frac{X_1 + X_2}{R_2 - R_1}(R_1X_2 - R_2X_1)} \tag{1}$$

$$\theta_1 = \frac{p\pi + \arctan\left(\dfrac{Z_1(R_1 - R_2)}{R_1X_2 - R_2X_1}\right)}{1 + r} \tag{2}$$

where: $p \in I$, $r = f_2/f_1$ with $r \geq 1$

$$G = R_{in1}/\left(R_{in1}^2 + X_{in1}^2\right) \tag{3}$$

$$B = X_{in1}/\left(R_{in1}^2 + X_{in1}^2\right) \tag{4}$$

where,

$$R_{in1} = \frac{R_1 Z_1^2\left[1 + \tan^2\theta_1\right]}{Z_1^2 - 2Z_1X_1\tan\theta_1 + \left(R_1^2 + X_1^2\right)\tan^2\theta_1} \tag{5}$$

$$X_{in1} = \frac{\left(Z_1^2 - R_1^2 - X_1^2\right)Z_1\tan\theta_1 + Z_1^2X_1\left[1 - \tan^2\theta_1\right]}{Z_1^2 - 2Z_1X_1\tan\theta_1 + \left(R_1^2 + X_1^2\right)\tan^2\theta_1} \tag{6}$$

3.2. Design of Section B

For an open stub to work at two frequencies, following set of equations must be satisfied:

$$jB = j\left(1/Z_2\right)\tan\theta_2 \tag{7}$$

$$-jB = j\left(1/Z_2\right)\tan(r\theta_2) \tag{8}$$

Z_2 and θ_2 are found by solving (7), (8) and they are given by:

$$\theta_2 = \frac{s\pi}{1+r}, \quad s \in I \tag{9}$$

$$Z_2 = \tan\theta_2/B \tag{10}$$

Similar to the way open stub was shown to work in dual-band mode, a short stub may be shown to work at two frequencies with design equations similar to (9)–(10), except that tangent in (10) is replaced by cotangent along with a minus sign.

After cancelling imaginary terms of Y_{in1} by using Y_{in2}, the impedance looking into combination of Sections A and B (and the load Z_L) is real and given by:

$$Z_{in3} = 1/G \,@\, f_1 \text{ and } @\, f_2 \tag{11}$$

3.3. Design of Section C

To match Z_{in3} with Z_0, the characteristic impedance of the required $\lambda/4$ line is given by, $Z_{DB-\lambda/4} = \sqrt{Z_0 Z_{in3}}$ [1]. This paper utilizes an L-type stepped impedance line [10] for dual-band functionality. However, there are other dual-band $\lambda/4$ transformers reported in literature [11]. Interestingly, this particular choice makes the implemented circuit look like that discussed in [8]. However, the two emanates from altogether different working principles. A distinguishing feature of the proposed scheme is its ability of utilizing the mirror image of Section C, shown in Figure 3, without any change in the design parameters. In contrast, the Monzon's transformer used in [8] cannot be replaced with its mirror image.

To derive the design equations, Figure 3(a) is considered. This network is modified form of the network discussed in [10], with $\alpha = \beta = \theta_4$, $Z_T = Z_{DB-\lambda/4}$, $Z_A = Z_4$ and $Z_B = Z_5$. With the

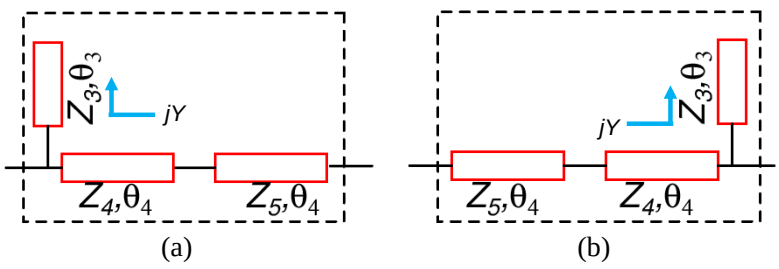

Figure 3. (a) Section C and (b) and its mirror image.

modification of Equations (6)–(8) reported in [10], the following design equations can be obtained to suit the present case:

$$Z_4 = Z_{DB-\lambda/4} \cot \theta_4 \tag{12}$$

$$Z_5 = Z_{DB-\lambda/4} \tan \theta_4 \tag{13}$$

$$Y = \frac{\cos 2\theta_4}{Z_{DB-\lambda/4} \cos^2 \theta_4} \tag{14}$$

And therefore, for network of Figure 3(a) to work as a dual-band $\lambda/4$ line, the electrical length θ_4 needs to be selected as follows.

$$\theta_4 = \frac{m\pi}{1+r}, \quad m \in I \tag{15}$$

Now, the remaining task is to design a dual band susceptance, Y, which can be easily designed using the methodology discussed in Section 3.2. The finalized expressions for this section are given below:

$$Z_{3,OC} = Z_{DB-\lambda/4} \frac{\cos^2 \theta_4}{\cos 2\theta_4} \tan \theta_3, \quad Z_{3,SC} = -Z_{DB-\lambda/4} \frac{\cos^2 \theta_4}{\cos 2\theta_4} \cot \theta_3 \tag{16}$$

$$\theta_3 = \frac{n\pi}{1+r}, \quad n \in I \tag{17}$$

where $Z_{3,OC}$ and $Z_{3,SC}$ are required characteristic impedances of open circuit stub and short circuit stubs, respectively.

Integers p, s, m, and n are chosen in view of compact size and realizable values of various transmission line sections.

To prove the claim that network of Figure 3(a) can well be substituted by its mirror image shown in Figure 3(b), one can proceed as follows.

The $ABCD$ parameter of network of Figure 3(b) is given by:

$$[ABCD]_{3(b)} = \begin{bmatrix} \cos\theta_4 & jZ_5 \sin\theta_4 \\ \dfrac{j\sin\theta_4}{Z_5} & \cos\theta_4 \end{bmatrix} \begin{bmatrix} \cos\theta_4 & jZ_4 \sin\theta_4 \\ \dfrac{j\sin\theta_4}{Z_4} & \cos\theta_4 \end{bmatrix} \begin{bmatrix} 1 & 0 \\ jY & 1 \end{bmatrix} \tag{18}$$

$$= \begin{bmatrix} \cos^2\theta_4 - \dfrac{Z_5}{Z_4}\sin^2\theta_4 - \dfrac{Y}{2}(Z_4+Z_5)\sin 2\theta_4 & \dfrac{1}{2}(Z_4+Z_5)\sin 2\theta_4 \\ j\left[\left(\dfrac{1}{Z_4}+\dfrac{1}{Z_5}\right)\dfrac{\sin 2\theta_4}{2} + Y\left(\cos^2\theta_4 - \dfrac{Z_4}{Z_5}\sin^2\theta_4\right)\right] & \cos^2\theta_4 - \dfrac{Z_4}{Z_5}\sin^2\theta_4 \end{bmatrix} \tag{19}$$

Now substituting the values of Z_4, Z_5 and Y from (12)–(14) results into following:

$$[ABCD]_{3(b)} = \begin{bmatrix} 0 & jZ_{DB-\lambda/4} \\ j\dfrac{1}{Z_{DB-\lambda/4}} & 0 \end{bmatrix} \tag{20}$$

Matrix in (20) represents $ABCD$ parameter of a quarter wave-line having characteristic impedance $Z_{DB-\lambda/4}$. This clearly justifies the claim that Section C of Figure 2 can be replaced by its mirror image and the design will work without altering the performance at the specified frequencies.

This finding should not be surprising considering that it is highly intuitive result. The procedure to show some network to be equivalent to a $\lambda/4$-line involves equating the network's $ABCD$ parameter to that of the $\lambda/4$-line. Since, the quarter-wave line is itself symmetric (having the same $ABCD$ parameter as that of its mirror image), the resulting network is also symmetric.

4. SIMULATION AND EXPERIMENTAL VERIFICATION

To test the proposed idea, in the first set of simulations, the two frequencies are kept fixed and load is varied arbitrarily as mentioned in Table 1. Simulation results are shown in Figure 4(a).

Next, an arbitrarily chosen frequency-dependent load as given by following function:

$$Z_L(f) = [a_1 + a_2(f - a_3)] + j\left[b_1 f^2 + b_2 f + b_3\right], \Omega \tag{21}$$

is considered, with $a_1 = 70$, $a_2 = 5E-9$, $a_3 = 1E9$, $b_1 = 2E-18$, $b_2 = 1E-9$ and $b_3 = 7$. With this load, design of the proposed network is carried out for three distinct values of $f_2 = 2.2\,\text{GHz}$, $2.4\,\text{GHz}$ and $2.6\,\text{GHz}$ while f_1 is fixed at $1\,\text{GHz}$. The simulated results are depicted in Figure 4(b). In this example, the value of r appears to be very limited; L-type dual-band $\lambda/4$ line was shown in [10] to work for $2 \leq r \leq 2.75$. It also reflects the flexibility of the proposed scheme that wherever a relatively wider range of r is required, T-type, PI-type, or other types of dual-band $\lambda/4$ line can be used [11]. As the next example, with the load still defined by (21), design is carried out by fixing $f_2 = 2.4\,\text{GHz}$, and taking three distinct values for $f_1 = 0.9\,\text{GHz}$, $1\,\text{GHz}$ and $1.1\,\text{GHz}$. The simulated results are shown in Figure 4(c).

A figure of merit for a matching network is the bandwidth around the centre frequencies. However, it is hard to evaluate the same for the case of FDCLs as the band-width hugely depends on how the load varies with frequency. It is also evident from (12)–(17) that once the value of r and the load at the two frequencies are known the design parameters of the matching network are fixed. Here comes the role of Z_{Tr_in}, the input impedance that the load sees into the transformer. It effectively regulates what kind of load variation can give higher bandwidth. It is important to remember that for complex conjugate matching, $\text{Re}(Z_{Tr\_in}) = \text{Re}(Z_L)$ and $\text{Im}(Z_{Tr\_in}) = -\text{Im}(Z_L)$, and therefore the wider the frequency span over which these two conditions are satisfied together, the wider is the bandwidth.

To illustrate and emphasize this point, case 1 and case 3 of the Table 1 is reconsidered. For the case 1, Figure 5(a) shows the variation of the real part of Z_L and that of Z_{Tr_in} with frequency whereas the variation of the imaginary parts of Z_L and that of Z_{Tr_in} with frequency is shown in the Figure 5(b). For the case 3, the corresponding plots appear in Figures 5(c) and 5(d). It can be observed from these plots that the variations in the real and imaginary parts at f_2 in case 3 are slower as compared to the corresponding variations in case 1 at both the frequencies and in case 3 at f_1. This is highlighted through the dotted boxes. This eventually leads to enhanced bandwidth in the case 3 at frequency f_2.

To show the usefulness of the proposed transformer further, input impedance, to be used as Z_L, of a commercial transistor is obtained from measured S-parameter data. Here, $Z_L(\Omega) = 19.465 + j1.482 \,@\, f_1$ and $20.466 + j18.792 \,@\, f_2$, where $f_1 = 1\,\text{GHz}$ and $f_2 = 2.42\,\text{GHz}$. Z_L is realized with the help of Vishay-Dale CRCW-series SMD resistors of $19.6\,\Omega$ and $20.5\,\Omega$ and lengths of transmission (to get inductive part). The proposed matching network is implemented on an FR-4 substrate ($\varepsilon_r = 4.7$, thickness $= 1.5\,\text{mm}$) with $35\,\mu\text{m}$ copper cladding.

Figure 6(a) shows both the fabricated prototypes. It is important to keep in mind that transformer

Table 1. The variation of the load impedance.

Frequency (GHz)	Z_L (Ω)		
	Case 1	Case 2	Case 3
$f_1 = 1$	$30 - j25$	$80 + j15$	$50 + j60$
$f_2 = 2.5$	$45 + j55$	$90 + j30$	$20 - j30$

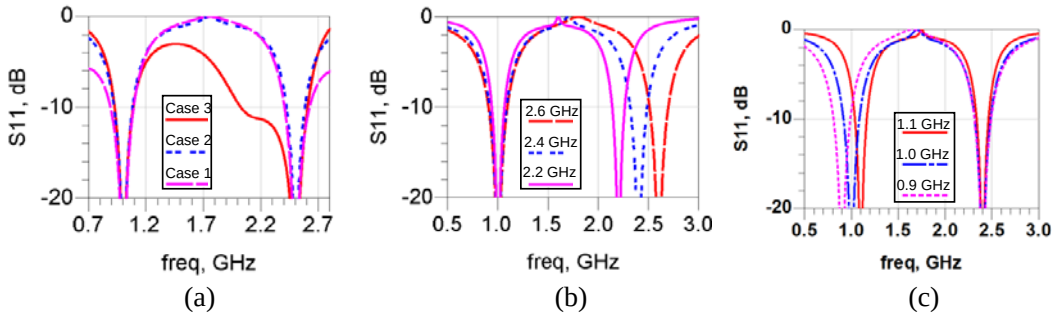

Figure 4. Simulation results. (a) Load varying but the frequencies fixed, (b) distinct loads as well as frequencies, f_1 fixed f_2 varying, and (c) f_2 fixed f_1 varying.

part is same in both the prototypes considering that it is a dual-band structure whereas the loads are changing with frequency. The simulated and measured results are shown in Figure 6(b). Measurements for both the prototypes were carried out around their respective centre frequencies. There seems to be a bit shift from the designed frequencies which is possibly due to slight inaccuracy in the model of the lumped resistor. Also, it may be noted that during the prototyping the loss due to SMA connectors have not been accounted for. Usually, the loss due to SMA at this low frequencies is not significant. Nevertheless, it is evident from the plots that the proposed network is working as a dual-frequency transformer with good performance. A comparison with the some state-of-the arts techniques appears in Table 2.

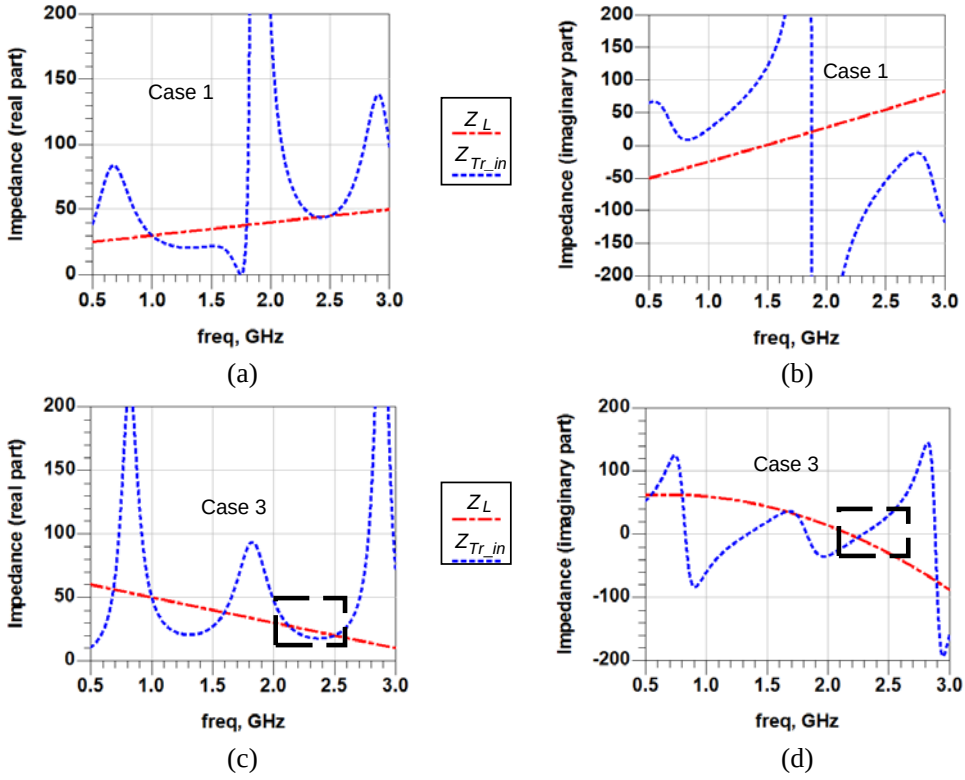

Figure 5. Variation of Z_L and Z_{Tr_in} with frequency for (a) real part, case 1, (b) imaginary part, case 1, (c) real part, case 3, (d) imaginary part, case 3. $f_1 = 1\,\text{GHz}$ and $f_2 = 2.5\,\text{GHz}$. All impedances are in Ω.

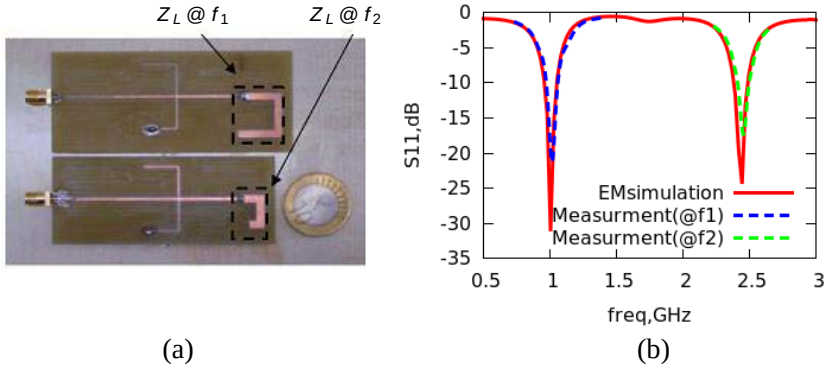

Figure 6. (a) Manufactured prototypes of the network shown in Figure 2. (b) Simulated and measured results.

Table 2. Comparison with some existing designs.

Technique/Ref. No	Type of Load	Experiment	Design Equations
2-Series lines [2]	Real	No	Simple
Chebyshev function [3]	Real	No	Simple
L-type network [4]	Real	Yes	Simple
3-Series lines [6]	FDCL	No	Simple
3-section lines + stubs [7]	FDCL	Yes	Complex[1]
1-section + stubs + Monzon's Transformer[2] [8]	FDCL	Yes	Simple
This work 1-section + stubs + DB-$\lambda/4$ line[3]	FDCL	Yes	Simple

[1]Need some tool for optimization.
[2]Some variables are free.
[3]No unique structure

5. CONCLUSION

A novel, simple and successful design methodology for realizing a dual-band matching network has been presented. It has been demonstrated that any dual-band quarter-wave line can be utilized for achieving dual-band impedance transformation for frequency dependent complex loads. The reported design also enables the use of mirror image of dual-band $\lambda/4$-line and which can potentially aid in achieving simpler board layout.

REFERENCES

1. Pozar, D. M., *Microwave Engineering*, 3rd Edition, J. Wiley & Sons, New Delhi, 2010.
2. Monzon, C., "A small dual-frequency transformer in two sections," *IEEE Trans. Microw. Theory Tech.*, Vol. 51, No. 4, 1157–1161, Apr. 2003.
3. Sophocles, J. and A. Orfanidis, "Two-section dual-band Chebyshev impedance transformer," *IEEE Microw. Wireless Comp. Lett.*, Vol. 13, No. 9, 382–384, Sep. 2003.
4. Park, M. J. and B. Lee, "Dual band design of single stub impedance matching networks with application to dual band stubbed T junctions," *Wiley Microwave & Optical Technology Letters*, Vol. 52, No. 6, 1359–1362, 2010.
5. Maktoomi, M. A. and M. S. Hashmi, "A coupled-line based L-section DC-isolated dual-band real to real impedance transformer and its application to a dual-band T-junction power divider," *Progress In Electromagnetics Research C*, Vol. 55, 95–104, 2014.
6. Liu, X., Y. Liu, S. Li, F. Wu, and Y. Wu, "A three-section dual-band transformer for frequency dependent complex load impedance," *IEEE Microw. Wireless Comp. Lett.*, Vol. 19, No. 10, 611–613, Oct. 2009.
7. Chuang, M.-L., "Dual-band impedance transformer using two-section shunt stubs," *IEEE Trans. Microw. Theory Tech.*, Vol. 58, No. 5, 1257–1263, May 2010.
8. Chuang, M.-L., "Analytical design of dual-band impedance transformer with additional transmission zero," *IET Microwaves, Antennas & Propagation*, Vol. 8, No. 13, 1120–1126, Oct. 2014.
9. Maktoomi, M. A., M. S. Hashmi, and F. M. Ghannouchi, "A T-section dual-band matching network for frequency-dependent complex loads incorporating coupled line with DC-block property suitable for dual-band transistor amplifiers," *Progress In Electromagnetics Research C*, Vol. 54, 75–84, 2014.
10. Cheng, K.-K. M. and F.-L. Wong, "A new Wilkinson power divider design for dual band application," *IEEE Microw. Wireless Comp. Lett.*, Vol. 17, No. 9, 664–666, Sep. 2007.

11. Rawat, K., M. S. Hashmi, and F. M. Ghannouchi, "Dual-band RF circuits and components for multi-standard software defined radios," *IEEE Circuits & Systems Magazine*, Vol. 12, No. 1, 12–32, First Quater 2012.